Improvement of superconducting properties in Na-doped *BSCCO* Superconductor

B. Özçelik[a*], M.Gürsul[a], A. Sotelo[b], M. A. Madre[b]

[a] *Department of Physics, Faculty of Sciences and Letters, Çukurova University. 01330 Adana, Turkey*
[b] *ICMA (CSIC-Universidad de Zaragoza). María de Luna, 3. 50018 Zaragoza, Spain.*

Abstract

In this study, the effect of Na substitution on the structural, electrical and magnetic properties of $Bi_2Sr_2Ca_{1-x}Na_xCu_2O_{8+y}$ superconductor with x=0.0, 0.05, 0.075, 0.1, 0.15, and 0.2 has been investigated. The effects of partial replacement of Na for Ca have been investigated by electrical resistivity (ρ-*T*), scanning electron microscopy (SEM), X-ray diffraction (XRD), and magnetic characterizations. XRD results have shown that the Bi-(2212) phase is the major one independently of the Na-concentration. SEM results indicate that the microstructure of samples is improved with increasing of Na-contents. From the electrical resistivity measurements it has been found that *Tc* is slightly higher than 92 K for Na-concentrations up to 0.20. Moreover, this trend is maintained in the magnetic measurements where the hysteresis loops are increased with increasing Na-concentrations. The maximum calculated *Jc*, using Bean's model, is around $10*10^6$ A/cm^2 at 10 K and ~ 1000 Oe for the 0.075 Na doped samples.

Keywords: Bi-based cuprates, XRD, SEM, Critical Current, M-H

***Corresponding Author:** Tel./fax:+90.322.3386060/2496/+90.322.3386070
e-mail: ozcelik@cu.edu.tr

1. Introduction

Since the discovery of Bi-based high-temperature superconductors [1], which are among the most promising materials for technological and industrial applications, many experimental studies have been performed [2-18] in order to improve their critical temperature (*Tc*), critical current density (*Jc*), and better understand the structural properties of the system. The BSCCO families can be described by the $Bi_2Sr_2Ca_{n-1}Cu_nO_{2n+4+y}$ general formula, where n=1, 2 and 3. The n value indicates the number of CuO_2 layers in the crystal structure, producing the Bi-2201, 2212 and 2223 phases with around 20, 85, and 110 K critical temperatures, respectively [19-21]. Among these phases, the Bi-2212 is stable in a wide range of compositions and processing temperatures but its *Tc* is influenced by the chemical composition. *Tc* increases significantly when the Bi and Ca contents are decreased, provided that the oxygen content is constant [22]. While BSCCO superconductors have some advantages as high critical temperature and magnetic field carrying capacity, they also have some disadvantages as the presence of weak-links, high anisotropy, and small coherence length which restrict them for technological applications. One of the most important problems in order to obtain high critical current density values is the presence of randomly oriented grains in the BSSCO system when it is processed by conventional techniques.

Generally, even very small misorientation of grains in these superconductors produces a negative effect on *Jc* values. For many years, researchers have tried to overcome those disadvantages and to improve their structural, mechanical and superconducting properties by using several techniques. Especially, one of the most useful techniques, in this regard, is the substitution of some elements at different cationic sites. These substitutions lead to important changes in charge carrier concentration and also release the restriction of spin alignment due to the spin lattice interaction [23]. The effect of such changes is one of the important features that help understanding the structural details and superconducting properties along with the mechanism of occurrence of superconductivity [24-26]. Besides chemical doping, the production techniques have also been widely studied by researchers to produce high quality and homogeneous samples. Among these preparation techniques, some of them can be underlined, as the classical solid state [27,28] melt quench [29-31], sol-gel [32-35] and the polymer matrix [36-38] methods.

The substitution of alkaline metals in the Bi-based superconductors has shown that the disorder produced by the cations incorporation in the crystal structure affects the T_C of the system, since their ionic radii (73–181 pm) overlap those of Bi, Sr, Ca, and Cu. Moreover,

alkaline metals have a +1 valence state; hence, their substitution is attractive from the point of changing carrier concentration. The effects of substituting alkaline metals for Bi, Sr, and Cu in BSCCO were studied by [39-41] and reported that while the *Tc* was increased by Li and Na doping, it was decreased by K and Rb. It was also found that alkaline metals drastically decreased the formation temperature of the Bi-2212 phase.

In previous works, the effects of several substitutions for Ca or Cu have been studied in detail [42-45]. On the other hand, in the best of our knowledge, no studies about the Na-substitution effect on the Bi-2212 properties have been made. As a consequence, the aims of the present work are:

(*i*) introducing optimum amounts of Na into the $Bi_2Sr_2Ca_{1-x}Na_xCu_2O_{8+y}$ system by replacing Ca due to their similar ionic radii but different oxidation state. Ca shows an oxidation state +2 while Na is +1. As a consequence, modifications can be produced in the crystal structure, together with changes in carrier concentration due to changes in oxygen content.

(*ii*) exploring the structural, electrical and magnetic behavior of these modified systems, compared with the undoped one.

(*iii*) evaluating the results as a function of Na-concentration, as all these mentioned effects should lead to modifications of the superconducting and magnetic properties of the system.

Moreover, a polymer solution method has been used to prepare the samples due to the following reasons: (a) the particle size is smaller than for the classical solid state method, leading to higher reactivity of powders, (b) Na_2CO_3, used for the solid state reaction, does not decompose at the treatment temperatures, only melts and it can be lost as a liquid phase during the thermal treatments, at least in a high proportion. As a consequence, it would be difficult to determine the substitution range, and (c) in the polymer solution method Na acetate is used (melting point ~ 328 ºC), but after coordination with polyethyleneimine (PEI) no sodium acetate can be found in the solution, as reported previously for the Cu acetate [36].

Finally, the modification of Bi-2212 ceramics induced by the Na-substitution for Ca has been determined by means of X-ray analysis (XRD), scanning electron microscopy (SEM) and magnetic measurements.

2. Experimental details

$Bi_2Sr_2Ca_{1-x}Na_xCu_2O_y$ samples, with x =0, 0.05, 0.075, 0.1, 0.15, and 0.20 have been prepared, by using a polymer matrix route described in detail elsewhere [15,46]. $Bi(CH_3COO)_3$ (≥99.99%, Aldrich), $Sr(CH_3COO)_2•0.5H_2O$ (99%, Panreac), $Ca(CH_3COO)_2•2H_2O$ (98%, Alfa Aesar), $Cu(CH_3COO)_2•H_2O$ (98%, Panreac) and $Na(CH_3COO)$ (99%, Alfa Aesar)

commercial powders were used as starting materials. They were weighed in stoichiometric amounts and dissolved in a mixture of glacial acetic acid (CH_3COOH) (Panreac PA) and distilled water. The use of a mixture of glacial acetic acid and water is due to the fact that in one side Sr acetate is insoluble in concentrated acetic acid and, on the other side, Bi acetate is not soluble in water [47]. Once a clear blue solution is obtained, polyethyleneimine (PEI) (Aldrich, 50 wt.% water) was added. The mixture becomes dark blue immediately reflecting the formation of Cu-N coordination bonds. The solution was then introduced into a rotary evaporator to reduce its volume (in ~80%), followed by heating on a hot plate at about 100 ºC for total solvent evaporation, producing a thermoplastic dark blue paste. Further heating at around 350 ºC produces a decomposition step (self combustion), as described schematically elsewhere [37], which produces the organic material decomposition. The resulting powder was then milled in an agate mortar and calcined twice at 750 and 800°C for 12 h, with an intermediate manual milling, in order to decompose the alkaline-earth carbonates.

Finally, the prereacted homogeneous powders were pressed into 13 mm diameter pellets, and thermally treated in order to produce the Bi-2212 superconducting phase. This process was performed under air, and consisted in two steps: 60 h at 860 ºC, followed by 12 h at 800 ºC and, finally, quenched in air to room temperature.

In order to identify the present phases, powder X-ray diffraction patterns of the materials were recorded at room temperature using a Rigaku D/max-B powder diffractometer system working with CuKα radiation and a constant scan rate between 2θ= 3-60º. The uncertainty of the crystal lattice parameters calculation remained in the ± 0.00001 range. SEM micrographs were taken using a LEO Evo-40 VPX scanning electron microscope fitted with an energy dispersive X-ray spectrometer (EDS). Magnetic measurements were carried out in a Quantum Design PPMS system. The $Bi_2Sr_2Ca_{1-x}Na_xCu_2O_{8+y}$ samples, with x =0, 0.05, 0.075, 0.1, 0.15, and 0.20 will be hereafter named as *Na-01, Na-02, Na-03, Na-04, Na-05*, and *Na-06*, respectively

3. Results and discussion

3.1 XRD characterization

In Fig.1, XRD patterns of all samples are shown. In the figure, the peaks corresponding to the Bi-2212 phase are indicated by +, and it is clear that all samples are mainly composed by the

Bi-2212 phase, independently of the Na amount. Moreover, minor peaks corresponding to the $CaCuO_2$ nonsuperconducting phase (identified by * in the figure) can be found in most of the samples. The crystal symmetry of all samples was determined to be tetragonal and the calculated lattice parameters using the least squares method are presented in Table 1. As it can be inferred from these data, while *a-b* parameters are slightly increasing, c-parameter is decreasing when Na-concentration is raised. These variations are due to the fact that the insertion of Na^{1+} substituting Ca^{2+} ions in the structure produces a decrease on the global positive charge in the structure. As a consequence, a modification on the oxygen content has to be produced to maintain the electrical neutrality in the structure, decreasing c-parameter and, consequently, raising the a-b. Additionally, it is found that there is no any phase transition in crystal symmetry with variation of Na concentration.

In order to get more information about the crystal sizes, the Debye Scherrer formula [48] has been applied to the XRD data, as:

$$L_{hkl} = 0.9\,\lambda / \beta\cos\theta \qquad (1)$$

where λ is the used wavelength, β is the full width at half maximum of X-ray peaks and θ is the angle of the peak. As can be seen from Table-1, the particle sizes increase with increasing Na-concentration, probably due to the decrease of the system melting point induced by Na. As a consequence, the growth process speed is increased due to the formation of a small amount of liquid phase.

3.2 SEM analysis

Fig. 2 shows the surface morphologies of all samples, which are composed of plate-like grains due to their preferential grain growth directions (along the ab planes). The Na-substituted samples possess bigger grain dimensions when compared with the undoped ones. The morphology of the particles, which appear as elongated platelets with no preferential orientation, is representative of samples and typical for solid state sintered materials. The amount of large and small grains is increased with raising Na-content, indicating that growth of large grains takes place at the expense of smaller grains. In fact, as the Na-content is increased from 0.05 to 0.2, large grains are observed to increase significantly in size, while small grains decrease accordingly, confirming the facts already discussed in the XRD section. During annealing Na-rich particles can form a liquid phase which improves the sintering process of the superconducting grains. It will be worthwhile to mention at this point that for the high Na-contents (above x=0.1), the partially molten regions could be observed. Further

Na substitutions produce deterioration of microstructure and, in fact, the amount of molten regions increase in an important manner (see SEM micrograph of sample *Na-06*).

3.3 Electrical measurements

The electrical resistivity (**ρ**) versus temperature (*T*) curves obtained from 110 K down to 60 K for all samples are displayed in Fig. 3. In this figure, it can be clearly seen that all samples possess very similar behavior over the onset critical temperature (T_c^{onset}) transition, with a metallic-like behavior, confirming that the Bi-2212 phase is the major one. Below the superconducting T_c^{onset} transition temperatures, the $\rho(T)$ curves show the typical behaviour of Bi-2212 superconductors, which have a relatively sharp decrease after T_c^{onset} transition temperatures. In addition, the normal state resistivity values (T_c^{onset}) for the Na-doped samples were found to be increased with increasing of Na-concentration compared with the pure one, *Na-01*, which can be associated to changes in hole concentration due to the incorporation of Na into the crystal structure. The sample *Na-06* has reached the highest critical temperature ~ 93.7 K. On the other hand, the offset transition temperature (T_c^{offset}) values slightly increase with raising Na-concentration (see Table 1). This trend in transition temperature values indicates the improved superconducting properties of the system with increasing Na-concentration. The onset and offset critical temperatures obtained from the normalized resistivity graph versus temperature are also shown in Table 1. On the other hand, the variation of ΔT_C (T_c^{onset} - T_c^{offset}) is decreased up to x=0.1 implying the improvement of grain sizes and the increasing of hole numbers, then indicates an incremental tendency while the Na-concentration increases. As a result, resistivity measurements also are in good agreement with SEM results.

3.4 Magnetic properties

The temperature dependence of zero field cooled (ZFC) magnetization of samples, measured under an external applied magnetic field of 50 Oe, are presented in Fig.4. In the ZFC measurements, the samples become diamagnetic below their onset temperatures and the diamagnetic saturation is almost reached at the lowest temperatures. Additionally, it can be concluded that the magnetizations show an incremental tendency on the superconducting properties with the raise of Na-concentration up to x=0.10. Then, the magnetization starts to decrease (for sample *Na-05*), pointing out the poorer superconducting properties in these samples. With increasing Na-concentration, the granular nature of BSCCO superconductor,

together with the effect of the weak connectivity at the grain boundaries, mainly causes this kind of behavior.

As it is well-known, the dc hysteresis cycles are very useful in determining the intragranular critical current density. Therefore, the magnetic-hysteresis cycles have been measured, between applied fields of ± 9 kOe, for all the samples, at 10K and represented in Fig.5. The magnetic-hysteresis loops indicate that the magnitude of magnetization effectively depends on Na-concentration levels. There is a clear raise of magnetization volume in the entire range of magnetic fields when Na-concentration is increased. It can be also clearly seen that the width of the hysteresis loops increases when the amount of Na is increased.

In addition, the diamagnetic behavior found in the M-H loops of all samples confirms the occurrence of conventional type-II superconductivity. Moreover, it is in agreement with the SEM observations which show an increase of the Na-substituted Bi-2212 phase when Na-concentration is raised. As a consequence of the higher amount of the Na-doped phase up to x=0.15, the superconducting properties or diamagnetic of these samples are improved. This behavior is a clear indication that the superconducting or diamagnetic properties of samples are positively affected when the Na-concentration is raised up to x=0.15, in agreement with SEM and resistivity results. Further, Na-doping above x=0.15 increases the Cooper pair breaking phenomena and then the magnetic properties of the samples diminish.

Fig. 6 shows the critical current density values, *Jc,* at 10 K calculated from M-H loops for all samples up to 1 T, obtained using the Bean's model [49];

$$Jc = 30\,\Delta M / d \qquad (2)$$

where *Jc* is the magnetization current density in ampéres per square centimeter of a sample. $\Delta M = M+ - M-$ is measured in electromagnetic units per cubic centimeter, and d is the thickness of the sample.

Calculated *Jc* of all samples effectively increases with the increasing magnetic field and Na-concentrations up to 0.1 T, and then starts to decrease. The important raise of *Jc* values for the Na-doped samples implies that the resistances to the flux creep of those samples are smaller due to the higher superconducting properties of Na-substituted Bi-2212 phase which do act as effective pinning centers. It is also well known that in the high-*T*c superconducting materials, non-superconducting impurity phases are highly effective in the flux-pinning mechanism. Due to the increase of impurities; the applied fields begin to significantly penetrate into the sample and decrease the critical current values. In this case, the high critical current density values are

the evidence of the strong pinning mechanism arising from Na-substitution. On the other hand, for high amount of Na, above x=0.15, an increase of non-superconducting impurities without pinning abilities is produced and, therefore, *Jc* values start to decrease.

4 Conclusions

In summary, a comparative study of physical and magnetic properties of Na-doped $Bi_2Sr_2Ca_{1-x}Na_xCu_2O_y$ samples prepared by polymer solution technique has been presented. X-ray diffraction, scanning electron microscopy, dc-resistivity, dc-magnetization and magnetic hysteresis studies have been performed to find the optimum Na-doping level. XRD suggests that samples with nearly single Bi-2212 phase have been produced, independently of the Na-concentration. The SEM micrographs confirm that while Na addition increases the grain sizes significantly, small grains decrease accordingly. All samples are predominantly composed by randomly oriented Bi-2212 plate-like grains, typical for solid state sintered materials. *R-T* results indicate that all samples exhibit metallic behavior above T_c^{onset}. From *M-H* measurements, it is found that the magnetization values and the volume of the closed hysteresis curves increase with increasing Na-concentration due to the formation of the Na-substituted Bi-2212 phase. Employing Bean's model, it is found that the increase on Na-concentrations produce a raise of *Jc* values. All the results point out that the above mentioned characteristics improve regularly with the rise of the Na-concentration up to a critical value of x=0.15. Further Na-addition leads to a decrease of superconducting properties.

Acknowledgements

This work is supported by Research Fund of Cukurova University, Adana, Turkey, under grant contracts no: FEF2013BAP22.

References

[1] H. Maeda, Y. Tanaka, M. Fukutomi, T. Asano, Jpn. J. Appl. Phys. 27, L209 (1988)

[2] B. Özçelik, H.Gündoğmuş, D.Yazıcı, J Mater Sci: Mater Electron 25, 2456 (2014)

[3] B. Özçelik, C. Kaya, H. Gündoğmuş, A. Sotelo, M.A. Madre, J Low Temp Phys**.** 174, 136 (2014)

[4] N. Türk, H. Gündogmus, M. Akyol, Z. D. Yakıncı, A. Ekicibil, B. Özçelik J Supercond Nov Magn27, 711 (2014)

[5] A. Özaslan, B. Özçelik, B. Özkurt, A. Sotelo,M.A. Madre, J Supercond Nov Magn 27, 53

(2014)

[6] H.Gündoğmuş, B. Özçelik, A. Sotelo, M. A. Madre J Mater Sci: Mater Electron 24, 2568, (2013)

[7] V. Lennikov, B. Özkurt, L. A. Angurel, A. Sotelo, B. Özçelik, G. F. de la Fuente, J Supercond.Nov.Magn. **26**, 947, (2013)

[8] B. Özçelik, B. Özkurt, M.E. Yakıncı, A. Sotelo, M. A. Madre, J Supercond Nov Magn. 26:873 (2013)

[9] D. Yazıcı, B. Ozçelik, M.E. Yakıncı, J. Low Temp. Phys. 163, 370 (2011)

[10] A. Sotelo, M. Mora, M. A. Madre, J. C. Diez, L. A. Angurel, G. F. de la Fuente, J. Eur. Ceram. Soc. 25, 2947 (2005)

[11] L. Jiang, Y. Sun, X. Wan, K. Wang, G. Xu, X. Chen, K. Ruan, J. Du: Physica C 300, 61 (1998)

[12] M. Zargar Shoushtari, S. E. Mousavi Ghahfarokhi: J.. Supercond. Nov. Magn. 24, 1505 (2011)

[13] A. I. Abou-Aly, M.M.H. Abdel Gawad, R. Awad, I. G-Eldeen: J. Supercond. Nov. Magn. 24, 2077 (2011)

[14] M. Mora, A. Sotelo, H. Amaveda, M. A. Madre, J. C. Diez, L. A. Angurel, G. F. de la Fuente, Bol. Soc. Esp. Ceram. V. 44, 199 (2005)

[15] G. F. de la Fuente, A. Sotelo, Y. Huang, M. T. Ruiz, A. Badia, L. A. Angurel, F. Lera, R. Navarro, C. Rillo, R. Ibañez, D. Beltran, F. Sapiña, A. Beltran, Physica C185, 509 (1991)

[16] B. Özkurt, M. A. Madre, A. Sotelo, M.E. Yakıncı, B. Özçelik, J. Supercond. Nov. Magn. 25, 799 (2012)

[17] S. Bal, M. Dogruer, G. Yıldırım, A. Varilci, C. Terzioglu, Y. Zalaoglu, J. Supercond. Nov. Magn. **25**, 847 (2012)

[18] B.Ozkurt, J Mater Sci: Mater Electron., 24, 2426 (2013)

[19] L.Gao, J. C. Huang, L. R. Meng, H. P. Hor, J.Bechtold, Y.Y. Sun, W. C. Chu, Z.Z. Sheng, M. A. Herman,: Nature 332, 623 (1988)

[20] W.C. Chu, J.Bechtold, L.Gao, H.P. Hor, J.C. Huang, L.R. Meng, Y.Y. Sun, Y.Q.Wang, Y.Y.Zue: Phys. Rev. Lett. 60,941 (1988)

[21] L.J. Tallon, G.R. Buckley, W.P.Gilbert, R.M.Presland, M.W.I. Brown, E.M. Bowder, A.L. Christian, R.Gafull: Nature 333, 153 (1988)

[22] P. Majewski, H. L. Su, M. Quilitz, J. Mater. Sci. 32, 5137, (1997)

[23] Y. Ando, A.N. Lavrov, S. Komiya, K. Segawa, X.F. Sun: Phys. Rev. Lett. 87:017001 (2001)

[24] J.M. Tarascon, P. Barboux, G.W. Hull, R. Ramesh, L.H. Greene, M. Gariod, M.S. Hedge, W. R. Mckinnon: Phys. Rev. B 38, 4316 (1989)

[25] H. Eisaki, N. Kaneko, D. Feng, L. Fengi, A. Damascelli, P.K. Mang, Z.X. Shen, M. Greven:Phys. Rev. B 69, 064512 (2004)

[26] K. Fujita, T, Noda, K.M. Kojima, H. Eisaki, S. Uchida: Phys. Rev. Lett. 95, 097006 (2005)

[27] N. Knauf, J. Harwischmacher, R. Miller, R. Borowski, B. Rodeu, D. Wohllebreu, Physica C 173, 414 (1991)

[28] M. F. Carrasco, F. M. Costa, R. F. Silva, F. Gimeno, A. Sotelo, M. Mora, J. C. Diez, L. A. Angurel, Physica C 415, 163 (2004)

[29] S. Elschner, J. Boch, G. Brommer, P. Hermann, IEEE Trans. Magn. 21, 2724 (1996)

[30] D. Yazici, B. Ozcelik, J. Supercond. Nov. Magn., 25, 293 (2012)

[31] D. Yazıcı, B. Ozcelik, S. Altın, M. E. Yakıncı, J.Supercond.Nov. Magn.,24, 217 (2011)

[32] C. J. Huang, T.Y. Tseng, T. S. Heh, F. H. Chen, W. S. Jong, Y. S. Fran, S. M. Shiau, Solid State Commun. 72, 563 (1989)

[33] R.S. Liu, W.N. Wang, C.T. Chang, P.T. Wu, Jpn. J. Appl. Phys. 28, L2155 (1989)

[34] T. Asaka, Y. Okazawa, T. Hirayama, K. Tachikawa, Jpn. J. Appl. Phys. 29, L280 (1990)

[35] A. Sotelo, M. A. Madre, Sh. Rasekh, J. C. Diez, L. A. Angurel, Adv. Appl. Ceram. 108, 285 (2009)

[36] A. Sotelo, G. F. de la Fuente, F. Lera, D. Beltran, F. Sapiña, R. Ibañez, A. Beltran, M. R. Bermejo, Chem. Mater. 5, 851 (1993)

[37] A. Sotelo, L. A. Angurel, M. T. Ruiz, A. Larrea, F. Lera, G. F. de la Fuente, Solid State Ionics 63, 883 (1993)

[38] A. Sotelo, J. I. Peña, L. A. Angurel, J. C. Diez, M. T. Ruiz, G. F. de la Fuente, R. Navarro, J. Mater. Sci. 32, 5679 (1997)

[39] L.D. Sykorova, O. Smrckova, V. Jakes, Phys. Stat. Sol. (C) **1**(7), 1952 (2004)

[40] T. Kawai, T. Horiuchi, K. Mitsui, K. Ogura, S. Takagi, S. Kawai, Physica C **161**, 561 (1989)

[41] O. Bilgili, Y. Selamet, K. Kocabas, J Supercond Nov Magn 21, 439 (2008)

[42] H. Gündogmus, B. Özçelik, B. Özkurt, A. Sotelo, M.A. Madre, J. Supercond. Nov. Magn, 26, 111(2013)

[43] C. Kaya, B. Özçelik, B. Özkurt, A. Sotelo, M.A. Madre, J Mater Sci:Mater Electron, 24, 1580 (2013)

[44] A.Ekicibil, A.Coşkun, B.Özçelik, K.Kıymaç Mod.Phys.Lett.B, **19** (6), 331 (2005)

[45] B.Özkurt, A.Ekicibil, M.A.Aksan, B.Özçelik, M E.Yakıncı, K.Kıymaç**,** Low Temp.Phys, **149**, No:1/2 October, 105 (2007)

[46] A. Sotelo, Sh. Rasekh, M.A. Madre, J.C. Diez: J. Supercond. Nov. Magn. 24, 19 (2011)

[47] D.R. Lide: CRC Handbook of Chemistry and Physics. CRC Press/Taylor and Francis, Boca Raton, FL (2010)

[48] B. D. Cullity, Element of X-ray Differaction, Addition-Wesley, Reading, MA (1978)

[49] C.P. Bean, Phys. Rev. Lett. 8, 250 (1962)

Table 1. T_c values deduced from the *R-T* measurement data, unit cell parameters, crystal size for each type of samples

Samples	***T_c(K)***	***ΔT(K)***	***Unit-cell parameter a=b (Å)***	***Unit-cell parameter c (Å)***	***L_{hkl}* (Å)**
Na-01	**T_c^{onset} =91.30** **$T_{c.}^{offset}$=80.07**	**11.23**	5.4280	30.7678	424.74
Na-02	**$T_{c.}^{onset}$=91.36** **$T_{c.}^{offset}$=81.55**	**9.81**	5.4283	30.7530	432.68
Na-03	**$T_{c.}^{onset}$=92.70** **$T_{c.}^{offset}$=82.80**	**9.90**	5.4336	30.7330	445.44
Na-04	**$T_{c.}^{onset}$= 92.42** **$T_{c.}^{offset}$=81.64**	**10.78**	5.4391	30.7322	446.85
Na-05	**$T_{c.}^{onset}$=92.56** **$T_{c.}^{offset}$=80.69**	**11.87**	5.4415	30.7318	450.45
Na-06	**$T_{c.}^{onset}$=93.69** **$T_{c.}^{offset}$=81.81**	**11.88**	5.4494	30.7290	463.68

Figure captions

Figure 1. XRD patterns of samples. In figure, *a-f* indicates the samples *Na01-Na06*, respectively. Peaks corresponding to the Bi-2212 and $CaCuO_2$ phases are indicated by + and *, respectively.

Figure 2. Representative SEM micrographs of samples surfaces

Figure 3. Dc electrical resistivity versus temperature curves for all samples between 60 and 110 K

Figure 4. Magnetization against temperature for samples with an applied field of 50 Oe

Figure 5. M-H curves for all samples measured at 10K

Figure 6. Calculated critical current densities, J_c, of the samples, as a function of the applied field, at 10K

Figure 1

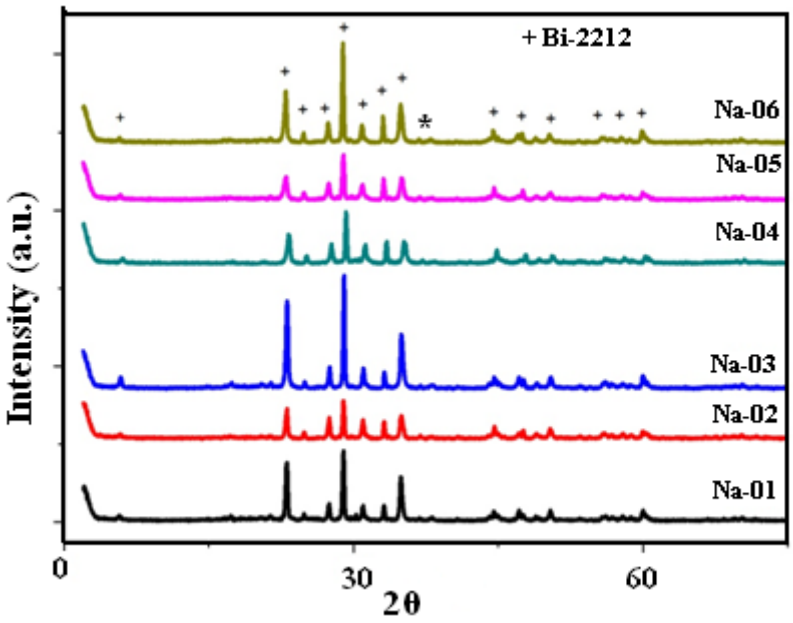

Figure 2

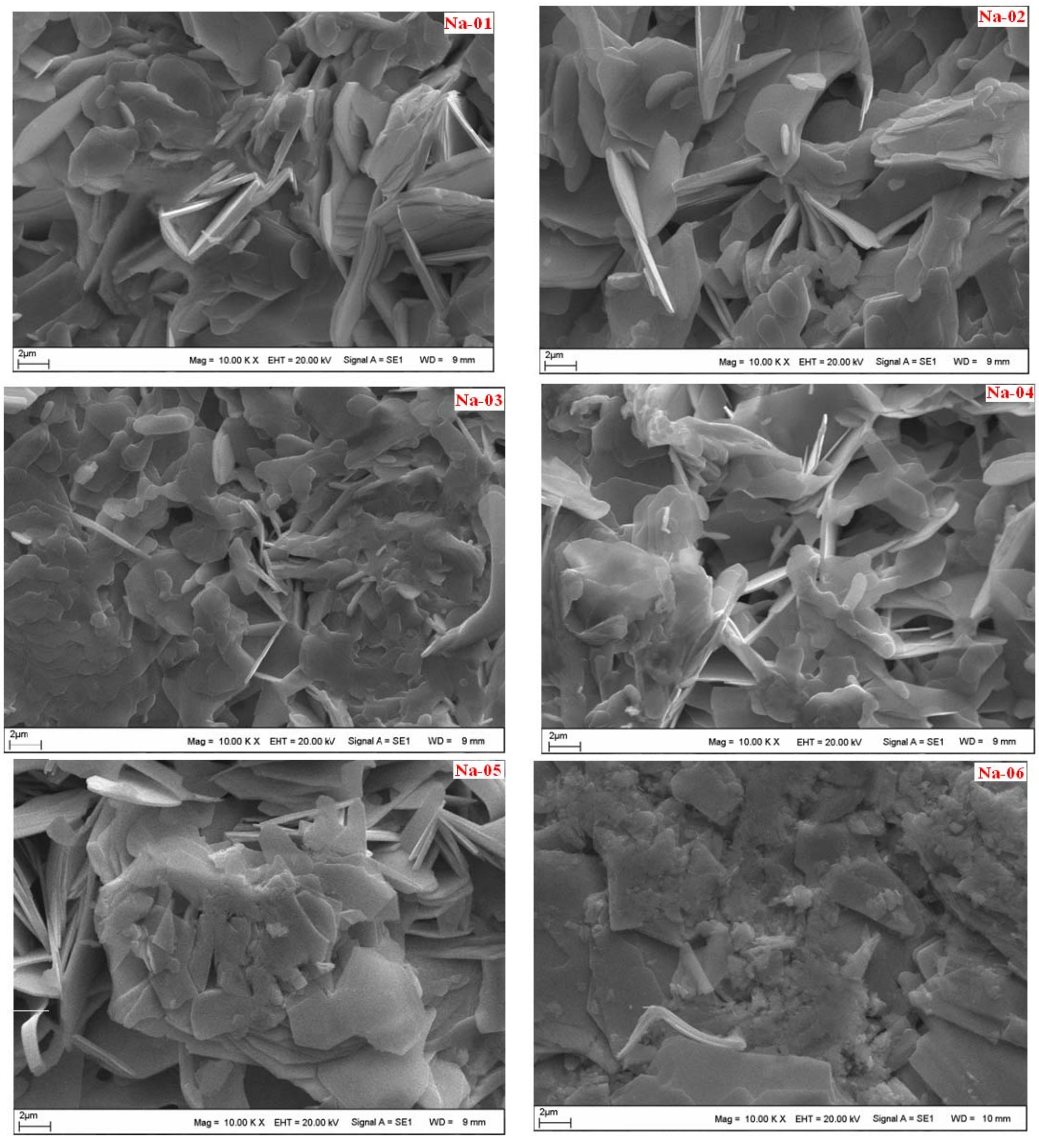
Na-01
2µm
Mag = 10.00 K X EHT = 20.00 kV Signal A = SE1 WD = 9 mm
Na-02
2µm
Mag = 10.00 K X EHT = 20.00 kV Signal A = SE1 WD = 9 mm
Na-03
2µm
Mag = 10.00 K X EHT = 20.00 kV Signal A = SE1 WD = 9 mm
Na-04
2µm
Mag = 10.00 K X EHT = 20.00 kV Signal A = SE1 WD = 9 mm
Na-05
2µm
Mag = 10.00 K X EHT = 20.00 kV Signal A = SE1 WD = 9 mm
Na-06
2µm
Mag = 10.00 K X EHT = 20.00 kV Signal A = SE1 WD = 10 mm

Figure 3

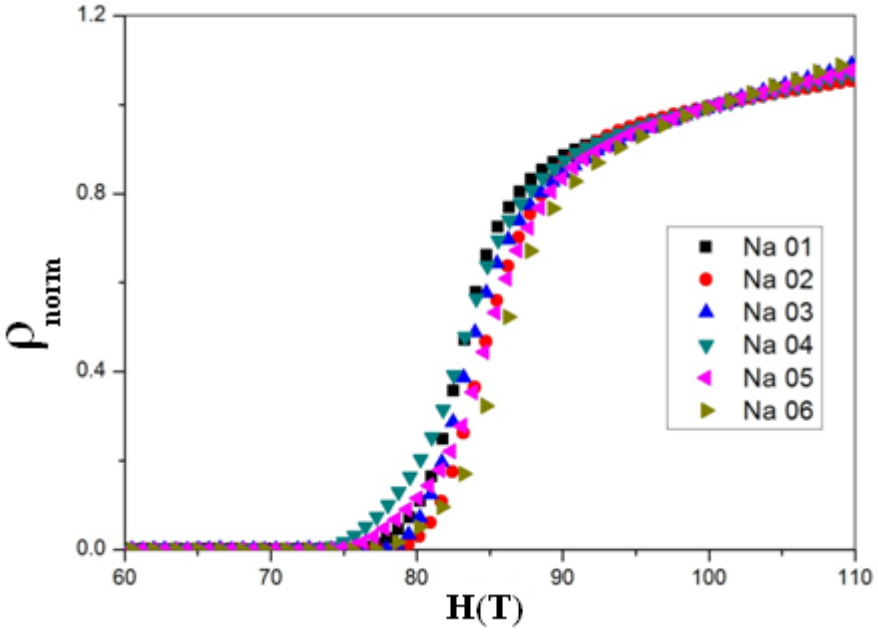
1.2
0.8
0.4
0.0
ρ norm
60
70
80
90
100
110
H(T)
Na 01
Na 02
Na 03
Na 04
Na 05
Na 06

Figure 4

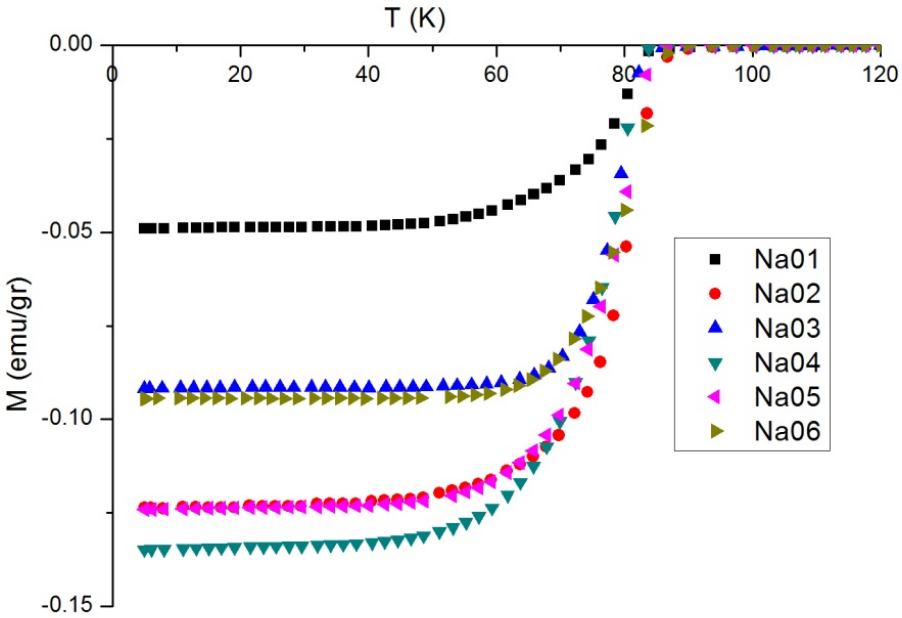
T (K)
0.00
-0.05
-0.10
-0.15
M (emu/gr)
0
20
40
60
80
100
120
Na01
Na02
Na03
Na04
Na05
Na06

Figure 5

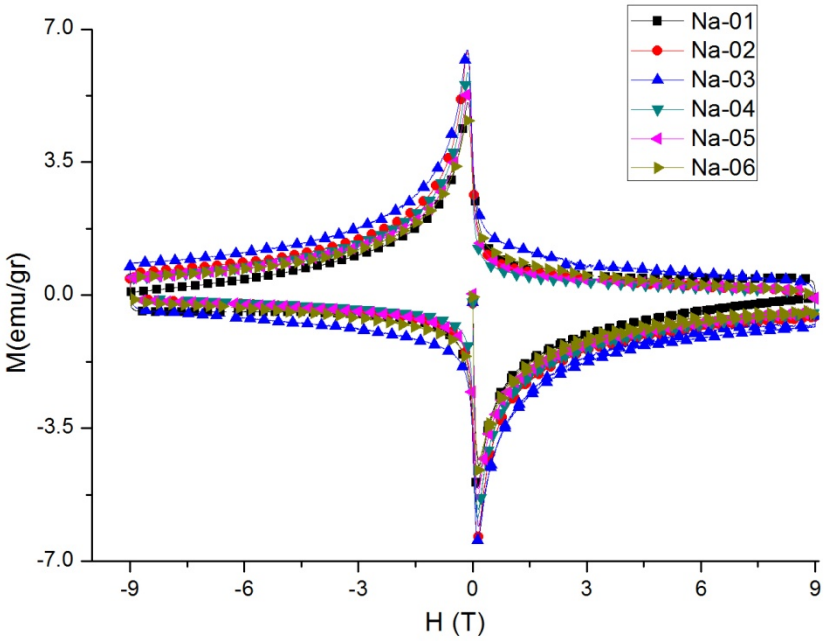

Figure 6

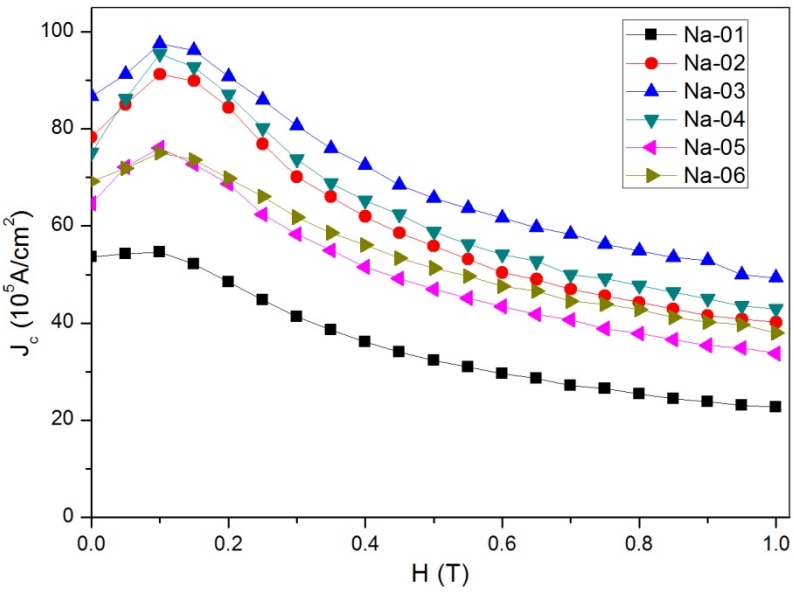
Na-01
Na-02
Na-03
Na-04
Na-05
Na-06
J_c (10^5A/cm^2)
H (T)
0
20
40
60
80
100
0.0
0.2
0.4
0.6
0.8
1.0